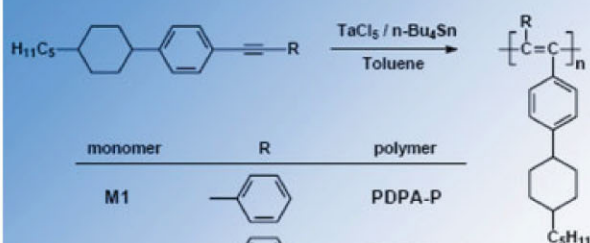
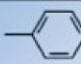
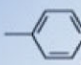
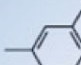

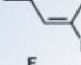


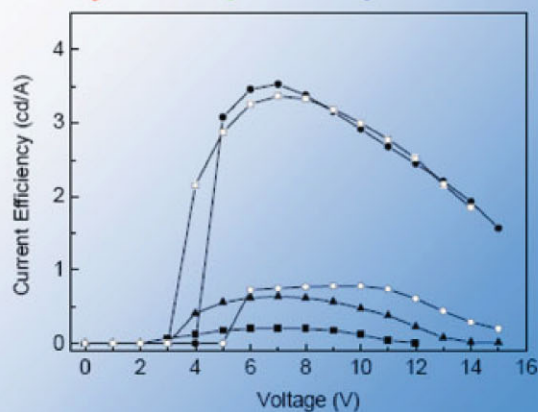
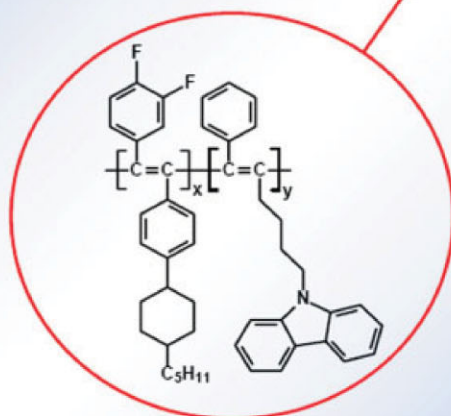
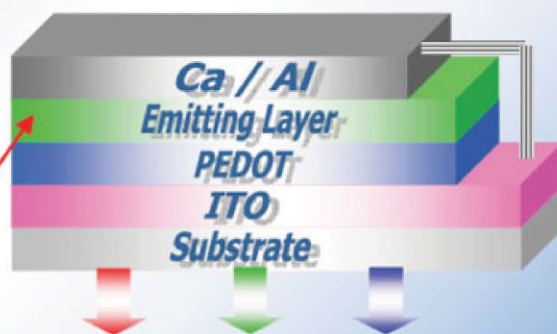
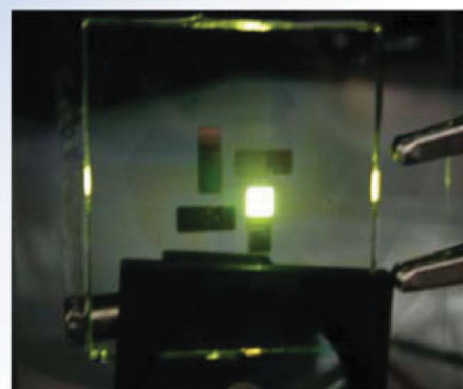
Special Series

New Frontiers in Functional Polymers

Highly Efficient Polyacetylene Derivatives for PLED Application



monomer	R	polymer
M1		PDPA-P
M2		PDPA-1F
M3		PDPA-2F
M4		PDPA-3F
M5		PDPA-5F



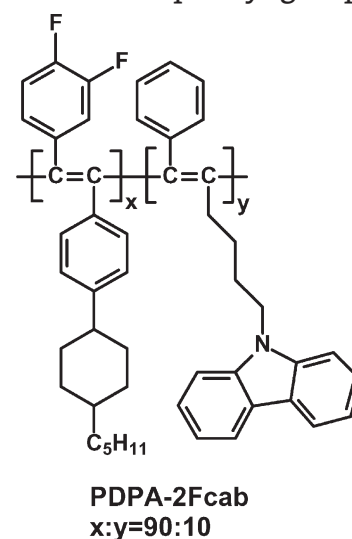
**Macromolecular
Chemistry
and Physics**

Further details on this special series
can be found at
www.mcp-journal.de

Synthesis and Electroluminescent Properties of Disubstituted Polyacetylene Derivatives Containing Multi-Fluorophenyl and Cyclohexylphenyl Side Groups

Sheng-Hsiung Yang, Chun-Hao Huang, Chiu-Hsiang Chen, Chain-Shu Hsu*

A new series of disubstituted polyacetylene derivatives that contain multi-fluorine atoms on the pendent phenyl ring have been synthesized and characterized. The results reveal a greater red-shift in UV-vis absorption and PL emission upon incorporating more fluorine atoms on the pendent phenyl ring. Among them, disubstituted polyacetylene with a difluorophenyl group (**PDPA-2F**) showed the highest luminescent efficiency. The device performance can be promoted by blending a hole-transporting material TM-TPD into **PDPA-2F** as the active layer or by using a light-emitting copolymer in which **PDPA-2F** was copolymerized with a carbazole group (**PDPA-2Fcab**). A light-emitting diode of ITO/PEDOT/**PDPA-2Fcab**/Ca/Al revealed a maximum luminescence of $4230 \text{ cd} \cdot \text{m}^{-2}$ at 14 V and a maximum current efficiency of $3.37 \text{ cd} \cdot \text{A}^{-1}$ at 7 V.



Introduction

Conjugated polymers have been extensively studied for their potential applications in light emitting diodes,^[1] organic lasers,^[2] thin film transistors,^[3] and solar cells.^[4] Polyacetylene (PA) is a prototype among many promising conjugated polymers, which exhibits high conductivity, and *n*- and/or *p*-type properties upon doping.^[5]

The conductivity of this polymer can reach as high as $10^5 \text{ S} \cdot \text{cm}^{-1}$ after doping.^[6] Although PA shows a very high electrical conductivity by doping, it has rarely been used as the light-emitting layer for electroluminescent (EL) devices. Non-substituted PA is insoluble, infusible, and unstable in air; almost no photoluminescence (PL) is observed in the visible region.

In the past few years, Masuda et al.,^[7–10] Tang et al.,^[11–14] and our laboratory^[15–17] have synthesized several series of substituted PA derivatives that are stable in air and soluble in common organic solvents. Although the conductivity of these PA derivatives is not as high as that of non-substituted PA, they show both PL and EL properties in the

S.-H. Yang, C.-H. Huang, C.-H. Chen, C.-S. Hsu
Department of Applied Chemistry, National Chiao Tung
University, 1001, Ta-Hsueh Road, Hsinchu 30010, Taiwan R.O.C.
Fax: +886-3-5131523; E-mail: cshsu@mail.nctu.edu.tw

visible wavelength region. Alkyl and phenyl groups are the most commonly used substituents for miscellaneous PA derivatives. These alkyl- and/or phenyl-substituted PAs emit blue to red light and have been used as active materials in polymer light emitting devices (PLED).^[16] For example, a single-layer device using poly(diphenylacetylene) (PDPA) as an emissive layer showed a stable green EL spectrum. However, the EL intensity is quite low.^[8]

Recently Masuda et al. have synthesized carbazole-substituted PAs using rhodium and tungsten as catalysts. These polymers exhibit photoconductivity and EL properties upon doping with an iridium complex.^[10] The best performance was reported with a multilayer EL device using poly[1-phenyl-5-(α -naphthoxy)pentyne] blended with poly(vinylcarbazole) (PVK) as the emitting layer, bathocuproine as a hole blocking layer, and 8-hydroxyquinoline aluminum (Alq3) as an electron transporting layer.^[12] A similar multilayer EL device using silole-containing PA as the active layer emitted blue-green light of 496 nm with a maximum brightness and current efficiency of 1118 cd · m⁻² and 1.45 cd · A⁻¹, respectively.^[13] Since then, the high-efficiency PA has not been explored for PLED application.

In this work, we aimed to synthesize a new series of disubstituted PAs with multifluorine substitution on the pendent phenyl ring. The effect of the number and substitution position of these fluorine atoms on energy levels and luminescent efficiency were examined. To further improve the device performance of these synthesized PAs, two approaches were proposed as well. One is based on a blend of PA and a hole transport material *N,N,N',N'*-tetra(4-methylphenyl)(1,1'-biphenyl)-4,4'-diamine (TM-TPD) as the emissive layer, while the other one is by incorporating a carbazole unit into the PA backbone by copolymerization.

Experimental Part

Characterization Methods

¹H NMR spectra were measured with a Varian 300 MHz spectrometer. Gel permeation chromatography (GPC) data assembled from a Viscotek T50A Differential Viscometer and a LR125 Laser Refractometer and three columns in series were used to measure the molecular weights of polymers relative to polystyrene standards at 35 °C. Infrared spectra were obtained by using a Perkin–Elmer Spectrum One spectrophotometer in the range of 400–4000 cm⁻¹. Differential scanning calorimetry (DSC) was performed on a Perkin–Elmer Pyris Diamond DSC instrument at a scan rate of 10 °C · min⁻¹. Thermal gravimetric analysis (TGA) was undertaken on a Perkin–Elmer Pyris 1 TGA instrument with a heating rate of 10 °C · min⁻¹. UV-Vis absorption spectra were

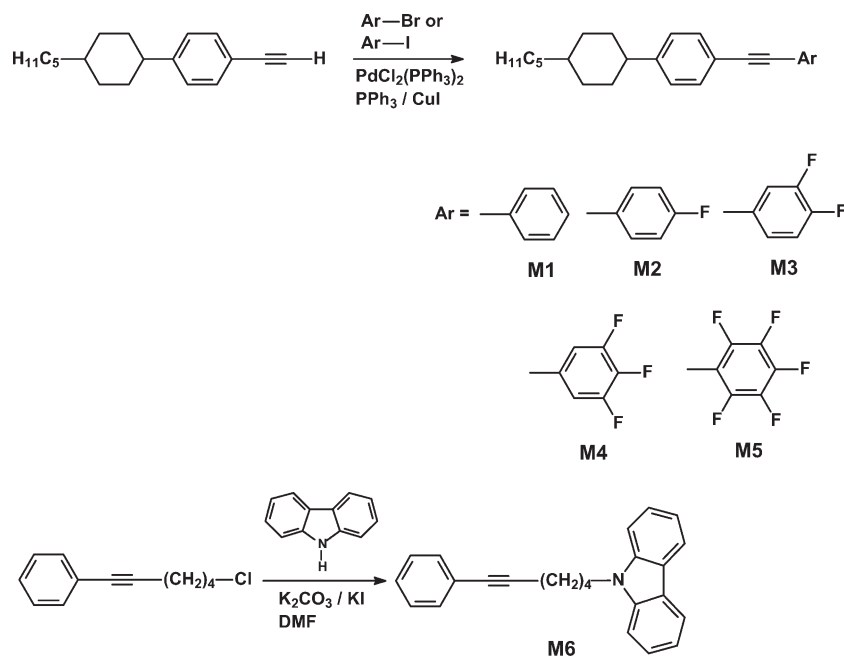
obtained with an HP 8453 diode array spectrophotometer. PL emission spectra were obtained using ARC SpectraPro-150 luminescence spectrometer. Cyclic voltammetric (CV) measurements were made in acetonitrile (CH₃CN) with 0.1 M tetrabutylammonium hexafluorophosphate (TBAPF₆) as the supporting electrolyte at a scan rate of 50 mV · s. Platinum wires were used as both the counter and working electrodes, and silver/silver ions (Ag in 0.1 M AgNO₃ solution, from Bioanalytical Systems, Inc.) were used as the reference electrode, and ferrocene was used as an internal standard. The corresponding highest-occupied molecular orbital (HOMO) and lowest-unoccupied molecular orbital (LUMO) energy levels were estimated from the onset redox potentials.

Synthesis of Monomers

All reagents and chemicals were purchased from commercial sources (Aldrich, Merck, Lancaster or TCI) and used without further purification. Anhydrous tetrahydrofuran (THF) and toluene were dried by distillation from sodium/benzophenone and calcium hydride, respectively. Scheme 1 depicts the syntheses of monomers **M1–M6**. Monomers **M2**, **M3**, and **M6** were synthesized according to the previous reports in the literature.^[18–20]

1-(4-(Pentylcyclohexyl)phenyl)-2-phenylacetylene (**M1**)

Iodobenzene (5.0 g, 24.5 mmol), PdCl₂(PPh₃)₂ (0.17 g, 0.25 mmol), CuI (0.24 g, 1.23 mmol), and PPh₃ (0.48 g, 1.84 mmol) were dissolved in triethylamine (50 mL) and the reaction mixture was stirred at room temperature under nitrogen. After all the catalysts were dissolved, 1-ethynyl-4-(4-pentylcyclohexyl)benzene (6.86 g, 27.0 mmol) was added and the mixture was refluxed at 70 °C for 12 h. After cooling to room temperature, triethylamine was removed under reduced pressure, and the crude product was



■ Scheme 1. Synthesis of monomers **M1–M6**.

extracted with ethyl acetate several times. The crude product was isolated by evaporating the solvent and purified by column chromatography (silica gel, hexane as eluent) to yield 6.87 g (86%) of white crystals; m.p. 54–55 °C. $^1\text{H NMR}$ (300 MHz, CDCl_3): $\delta = 0.88$ (t, $J = 7.2$ Hz, 3H), 1.04–1.47 (m, 13H), 1.87 (d, $J = 10.5$ Hz, 4H), 2.4 (t, $J = 12$ Hz, 1H), 7.19 (d, $J = 7.2$ Hz, 2H), 7.34 (m, 5H), 7.38 (d, $J = 7.2$ Hz, 2H).

$^{13}\text{C NMR}$ (75 MHz, CDCl_3): $\delta = 12.38, 22.71, 26.63, 32.19, 33.45$ (2C), 34.09 (2C), 37.25, 37.72, 44.09, 89.5 (C \equiv C), 90.4 (C \equiv C), 119.38 (1C, Ar), 125.6 (1C, Ar), 127.02 (2C, Ar), 128.35 (2C, Ar), 131.55 (2C, Ar), 131.64 (2C, Ar), 148.56 (1C, Ar).

IR (KBr): 3 030, 2 954, 2 924, 2 846, 2 221, 1 597, 1 511, 1 467, 1 442, 1 375, 1 214, 1 069, 966, 896, 828, 754 cm^{-1} .

MS (EI-MS): $m/z = 330.5$.

$\text{C}_{25}\text{H}_{30}$: Calcd. C 90.85, H 9.15; Found C 90.8, H 9.2.

1-(3,4,5-Trifluorophenyl)-2-(4-(pentylcyclohexyl)phenyl)acetylene (**M4**)

By following the synthetic procedure for **M1** and using 3,4,5-trifluoroiodobenzene as starting material, the compound **M4** was obtained as white crystals (83% yield); m.p. 60–62 °C. $^1\text{H NMR}$ (300 MHz, CDCl_3): $\delta = 0.87$ (t, $J = 7.2$ Hz, 3H), 1.04–1.47 (m, 13H), 1.86 (d, $J = 10.5$ Hz, 4H), 2.46 (t, $J = 12$ Hz, 1H), 7.08 (m, 2H), 7.12 (d, $J = 7.2$ Hz, 2H), 7.42 (d, $J = 7.2$ Hz, 2H).

$^{13}\text{C NMR}$ (75 MHz, CDCl_3): $\delta = 12.38, 22.71, 26.63, 32.19, 33.45$ (2C), 34.09 (2C), 37.25, 37.32, 44.09, 85.61 (C \equiv C), 91.2 (C \equiv C), 115.61 (1C, Ar), 115.91 (1C, Ar), 119.38 (1C, Ar), 127.02 (2C, Ar), 131.64 (2C, Ar), 138.38 (1C, Ar), 141.96 (1C, Ar), 143 (1C, Ar), 149.16 (1C, Ar), 152.3 (1C, Ar).

IR (KBr): 3 030, 2 957, 2 922, 2 852, 2 682, 2 217, 1 909, 1 609, 1 529, 1 447, 1 428, 1 379, 1 255, 1 206, 1 202, 1 070, 1 046, 980, 910, 856, 832.

MS (EI-MS): $m/z = 384.4$.

$\text{C}_{25}\text{H}_{27}\text{F}_3$: Calcd. C 78.1, H 7.08; Found C 77.9, H 7.12.

1-(2,3,4,5,6-Pentafluorophenyl)-2-(4-(pentylcyclohexyl)phenyl)acetylene (**M5**)

By following the synthetic procedure for **M1** and using 2,3,4,5,6-pentafluoroiodobenzene as starting material, the compound **M5** was obtained as white crystals (84% yield); m.p. 73–75 °C. $^1\text{H NMR}$ (300 MHz, CDCl_3): $\delta = 0.87$ (t, $J = 7.2$ Hz, 3H), 1.01–1.48 (m, 13H), 1.86 (d, $J = 11.5$ Hz, 4H), 2.48 (t, $J = 12$ Hz, 1H), 7.18 (d, $J = 7.2$ Hz, 2H), 7.48 (d, $J = 7.2$ Hz, 2H).

$^{13}\text{C NMR}$ (75 MHz, CDCl_3): $\delta = 14.09, 22.63, 26.64, 30.87, 32.21$ (2C), 34.45 (2C), 37.25, 37.33, 44.68, 72.36 (C \equiv C), 100 (1C, Ar), 101.97 (C \equiv C), 118.8 (1C, Ar), 126.82 (2C, Ar), 131.47 (2C, Ar), 136.1 (2C, Ar), 139.31 (2C, Ar), 142.82 (1C, Ar), 145.17 (1C, Ar), 148.93 (1C, Ar), 149.91 (1C, Ar).

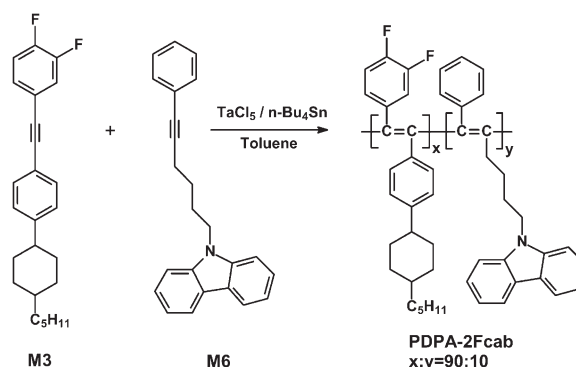
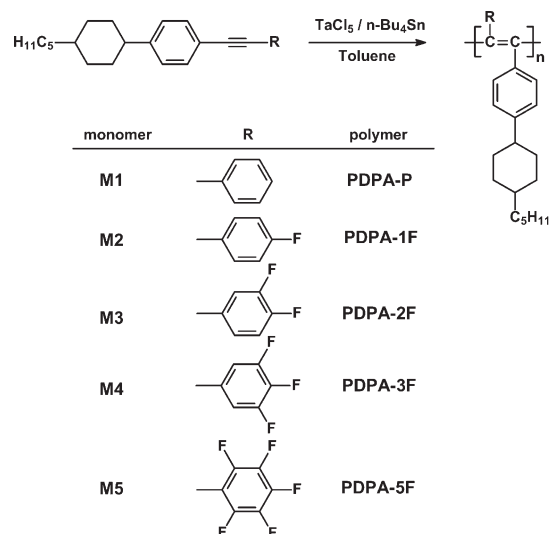
IR (KBr): 3 030, 2 957, 2 920, 2 854, 2 230, 1 917, 1 622, 1 525, 1 496, 1 445, 1 412, 1 365, 1 109, 1 096, 1 029, 984, 967, 835.

MS (EI-MS): $m/z = 420.4$.

$\text{C}_{25}\text{H}_{25}\text{F}_5$: Calcd. C 71.41, H 5.99; Found C 71.9, H 5.82.

Synthesis of Polymers

Scheme 2 depicts the synthetic routes for homopolymers **PDPA-P**, **PDPA-1F**, **PDPA-2F**, **PDPA-3F**, **PDPA-5F**, and a copolymer **PDPA-**



Scheme 2. Synthesis of homopolymers **PDPA-P**, **PDPA-1F**, **PDPA-2F**, **PDPA-3F**, **PDPA-5F**, and the copolymer **PDPA-2Fcab**.

2Fcab. The polymerization was carried out using TaCl_5 as catalyst and $n\text{-Bu}_4\text{Sn}$ as co-catalyst in anhydrous toluene. All experimental operations were performed in a glove-box, except for the purification of the polymers, which was done in the open atmosphere. An experimental procedure for the polymerization of **M1** is given below. A mixture of TaCl_5 (0.158 g, 0.4 mmol) and $n\text{-Bu}_4\text{Sn}$ (0.28 mg, 0.8 mmol) in anhydrous toluene (10 mL) was heated at 80 °C for 30 min. A solution of monomer **M1** (0.9 g, 4.12 mmol) in anhydrous toluene (10 mL) was then added. The resulting mixture was continuously stirred and heated at 80 °C for 24 h. After cooling to room temperature, the solution was poured into methanol and the product filtered off. The polymer was purified by dissolving the crude product in THF and re-precipitated from methanol several times. After drying under vacuum for 24 h, the final polymer **PDPA-P** was obtained as a yellow solid (0.61 g, 81%). $^1\text{H NMR}$ (300 MHz, CDCl_3): $\delta = 0.88$ (t, $J = 7.2$ Hz, 3H), 1.04–1.47 (m, 13H), 1.87 (d, $J = 10.5$ Hz, 4H), 2.4 (t, $J = 12$ Hz, 1H), 7.19 (d, $J = 7.2$ Hz, 2H), 7.34 (m, 5H), 7.38 (d, $J = 7.2$ Hz, 2H).

$^{13}\text{C NMR}$ (75 MHz, CDCl_3): $\delta = 12.38, 22.71, 26.63, 32.19, 33.45$ (2C), 34.09 (2C), 37.25, 37.32, 44.09, 119.38 (1C, Ar), 125.6 (1C, Ar), 127.02 (2C, Ar), 128.35 (2C, Ar), 131.55 (2C, Ar), 131.64 (2C, Ar), 148.56 (1C, Ar), 156.02 (2C, C=C).

$\text{C}_{25}\text{H}_{30}$: Calcd. C 90.85, H 9.15; Found C 89.55, H 8.89.

PDPA-1F

Yield 92%. ^1H NMR (300 MHz, CDCl_3): δ = 0.88 (t, J = 7.2 Hz, 3H), 1.04–1.47 (m, 13H), 1.85 (d, J = 10.5 Hz, 4H), 2.41 (t, J = 12 Hz, 1H), 7.11 (m, 2H), 7.17 (d, J = 7.2 Hz, 2H), 7.43 (d, J = 7.2 Hz, 2H), 7.55 (m, 2H).

^{13}C NMR (75 MHz, CDCl_3): δ = 12.38, 22.71, 26.63, 32.19, 33.45 (2C), 34.09 (2C), 37.25, 37.32, 44.09, 115.69 (1C, Ar), 115.85 (1C, Ar), 117.2 (2C, Ar), 119.38 (1C, Ar), 127.02 (2C, Ar), 131.64 (2C, Ar), 141.96 (1C, Ar), 143 (1C, Ar), 149.16 (1C, Ar), 154.52 (2C, C=C).

$\text{C}_{25}\text{H}_{29}\text{F}$: Calcd. C 86.16, H 8.39; Found C 86.01, H 8.35.

PDPA-2F

Yield 96%. ^1H NMR (300 MHz, CDCl_3): δ = 0.87 (t, J = 7.2 Hz, 3H), 1.08–1.47 (m, 13H), 1.87 (d, J = 10.5 Hz, 4H), 2.57 (t, J = 12 Hz, 1H), 7.09 (m, 2H), 7.13 (d, J = 7.4 Hz, 2H), 7.16 (s, 1H), 7.41 (d, J = 7.2 Hz, 2H).

^{13}C NMR (75 MHz, CDCl_3): δ = 12.38, 22.61, 26.63, 32.19, 33.24 (2C), 34.12 (2C), 37.25, 37.32, 44.09, 115.75 (1C, Ar), 115.85 (1C, Ar), 116.1 (1C, Ar), 119.38 (1C, Ar), 126.82 (2C, Ar), 131.34 (2C, Ar), 137.38 (1C, Ar), 141.96 (1C, Ar), 143.3 (1C, Ar), 149.26 (1C, Ar), 155.24 (2C, C=C).

$\text{C}_{25}\text{H}_{28}\text{F}_2$: Calcd. C 81.93, H 7.7; Found C 81.54, H 7.4.

PDPA-3F

Yield 90%. ^1H NMR (300 MHz, CDCl_3): δ = 0.87 (t, J = 7.2 Hz, 3H), 1.04–1.47 (m, 13H), 1.92 (d, J = 10.3 Hz, 4H), 2.48 (t, J = 12 Hz, 1H), 7.09 (m, 2H), 7.14 (d, J = 7.2 Hz, 2H), 7.46 (d, J = 7.1 Hz, 2H).

^{13}C NMR (75 MHz, CDCl_3): δ = 12.38, 22.71, 26.63, 32.19, 33.45 (2C), 34.09 (2C), 37.25, 37.32, 44.09, 115.61 (1C, Ar), 115.9 (1C, Ar), 119.38 (1C, Ar), 127.02 (2C, Ar), 131.64 (2C, Ar), 138.78 (1C, Ar), 141.96 (1C, Ar), 143 (1C, Ar), 149.2 (1C, Ar), 152.5 (1C, Ar), 154.64 (2C, C=C).

$\text{C}_{25}\text{H}_{27}\text{F}_3$: Calcd. C 78.1, H 7.08; Found C 77.61, H 6.83.

PDPA-5F

Yield 31%. ^1H NMR (300 MHz, CDCl_3): δ = 0.88 (t, J = 7.2 Hz, 3H), 1.1–1.48 (m, 13H), 1.86 (d, J = 11.5 Hz, 4H), 2.46 (t, J = 12 Hz, 1H), 7.16 (d, J = 7.2 Hz, 2H), 7.45 (d, J = 7.2 Hz, 2H).

^{13}C NMR (75 MHz, CDCl_3): δ = 14.09, 22.63, 26.64, 30.87, 32.21 (2C), 34.45 (2C), 37.25, 37.33, 44.68, 100 (1C, Ar), 118.8 (1C, Ar), 126.82 (2C, Ar), 131.47 (2C, Ar), 136.1 (1C, Ar), 139.31 (1C, Ar), 142.82 (1C, Ar), 145.17 (1C, Ar), 148.93 (1C, Ar), 149.91 (1C, Ar), 154.1 (2C, C=C).

$\text{C}_{25}\text{H}_{25}\text{F}_5$: Calcd. C 71.41, H 5.99; Found C 70.94, H 5.53.

PDPA-2Fcab

Yield 90%. ^1H NMR (300 MHz, CDCl_3): δ = 0.87 (t, J = 7.2 Hz, 3H), 1.08–1.47 (m, 13H), 1.87 (d, J = 10.5 Hz, 4H), 2.57 (t, J = 12 Hz, 1H), 7.09 (m, 2H), 7.13 (d, J = 7.4 Hz, 2H), 7.16 (s, 1H), 7.41 (d, J = 7.2 Hz, 2H).

^{13}C NMR (75 MHz, CDCl_3): δ = 12.38, 22.61, 26.63, 32.19, 33.24 (2C), 34.12 (2C), 37.25, 37.32, 44.09, 115.75 (1C, Ar), 115.85 (1C, Ar), 116.1 (1C, Ar), 119.38 (1C, Ar), 126.82 (2C, Ar), 131.34 (2C, Ar), 137.38 (1C, Ar), 141.96 (1C, Ar), 126.82 (2C, Ar), 131.34 (2C, Ar), 137.38 (1C, Ar), 141.96 (1C, Ar), 143.3 (1C, Ar), 149.26 (1C, Ar), 155.24 (2C, C=C).

$\text{C}_{249}\text{H}_{273}\text{F}_{18}\text{N}$: Calcd. C 82.53, H 7.65, N 0.39; Found C 80.81, H 7.91, N 0.78.

Device Fabrication and Measurement

Double-layer EL devices were fabricated as sandwich structures between a calcium (Ca) cathode and an indium-tin oxide (ITO) anode. An ITO-coated glass substrate was pre-cleaned and treated with UV/ozone before use. The poly(ethylene 3,4-dioxythiophene): polystyrene sulfonate (PEDOT:PSS) purchased from Bayer was then spin-coated and annealed at 150 °C for 1 h under vacuum as the hole injection layer. The thickness of the PEDOT:PSS layer was ca. 50 nm. An emissive layer was then spin-coated from its chloroform solution on top of the PEDOT layer to give a thin film with a thickness of ≈ 70 nm. Finally, a layer of Ca (35 nm) and aluminum (100 nm) was thermally evaporated on top of the emissive layer at base pressures lower than 6×10^{-7} Torr. The active device area was 4 mm². The current density–voltage–luminance characteristics were measured under ambient conditions using a Keithley 2400 source meter and a PR-650 spectrophotometer.

Results and Discussion**Synthesis of Polymers**

As mentioned in the experimental part, all polymerizations were carried out at 80 °C in anhydrous toluene, using TaCl_5 as catalyst and $n\text{-Bu}_4\text{Sn}$ as co-catalyst. The polymerization conditions are mild and the molecular weights of the obtained polymers are relatively large. Table 1 summarizes the molecular weights and polydispersity index (PDI) of the resulting polymers. The weight-average molecular weights (\overline{M}_w) of these polymers are in the range from 7.5×10^4 to 141.7×10^4 , and the PDI ($\overline{M}_w/\overline{M}_n$) is less than 2. Among them, **PDPA-5F** has the lowest yield and

Table 1. Polymerization results and thermal properties of polymers **PDPA-P**, **PDPA-1F**, **PDPA-2F**, **PDPA-3F**, and **PDPA-5F**.

Polymer	\overline{M}_n ($\times 10^4$)	\overline{M}_w ($\times 10^4$)	PDI	T_g	T_d
				°C	°C
PDPA-P	30.6	42.6	1.39	202	415
PDPA-1F	76.2	127.2	1.67	220	401
PDPA-2F	89.1	141.7	1.59	233	410
PDPA-3F	72.6	123.4	1.70	236	425
PDPA-5F	4.2	7.5	1.78	231	400

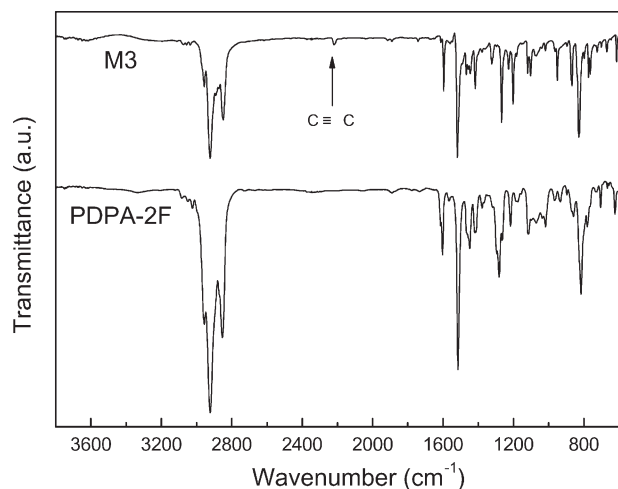


Figure 1. FT-IR spectra of monomer **M3** and the corresponding polymer **PDPA-2F**.

molecular weights; this could be a result of the pentafluoro substitution which withdraws partial electron densities from the triple bond and thus affects the polymerization. All the obtained polymers can be dissolved in common organic solvents, such as chloroform, toluene, and chlorobenzene. Transparent and self-standing films can be cast from their solutions.

Figure 1 shows the FT-IR spectra of monomer **M3** and its corresponding polymer **PDPA-2F**. The characteristic band centered at 2220 cm^{-1} was assigned to the $\text{C}\equiv\text{C}$ stretching in **M3**, and it totally diminished in the spectrum of **PDPA-2F**. Instead, a new absorption band located at 1650 cm^{-1} was formed, which was assigned to $\text{C}=\text{C}$ stretching in the main chain. The GPC and FT-IR observations revealed that **PDPA-2F** was successfully synthesized.

Thermal Properties

The glass transition temperature (T_g) and thermal decomposition temperature (T_d) of the synthesized PAs are also summarized in Table 1. The T_d value is defined as the temperature for 5% weight loss. These polymers show good thermal stabilities with a high T_g ($>200\text{ }^\circ\text{C}$) and a high T_d ($>400\text{ }^\circ\text{C}$), which are important advantages in the fabrication of light-emitting devices. The T_g of fluorinated polymers **PDPA-1F**, **PDPA-2F**, **PDPA-3F**, and **PDPA-5F** is higher than that of **PDPA-P**, which indicates that fluorine substitution can improve thermal stabilities. In addition, **PDPA-3F** has the highest T_d up to $425\text{ }^\circ\text{C}$.

Optical Properties

Figure 2 shows the UV-vis absorption spectra of five PA derivatives in the thin film state. The UV-vis spectrum of

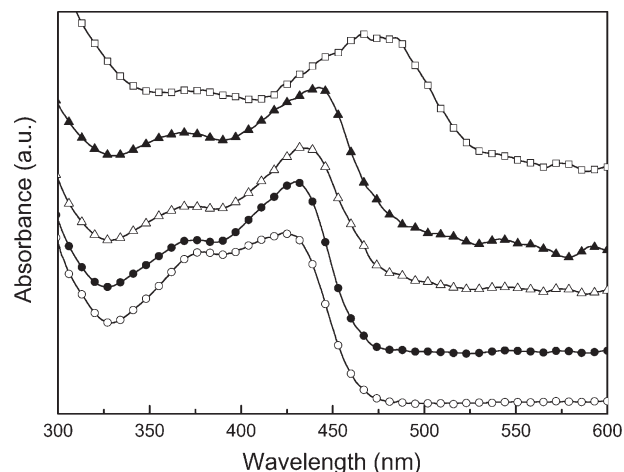


Figure 2. UV-vis absorption spectra of polymers **PDPA-P** (○), **PDPA-1F** (●), **PDPA-2F** (△), **PDPA-3F** (▲), and **PDPA-5F** (□) in the thin film state.

PAs often shows two absorption bands that belong to a $\pi-\pi^*$ inter-band transition along the conjugated main chain.^[15] It is seen that a continuous red-shift of the absorption band occurs as the number of fluorine atom increases, from 423 to 473 nm. A similar observation is also observed in the PL emission spectra, as shown in Figure 3. The maximum emission band is red-shifted from 517 nm (**PDPA-P**) to 568 nm (**PDPA-5F**). The UV-vis absorption and PL emission maxima of all polymers in different states are summarized in Table 2. It is well-known that the fluorine atom has a high electron affinity and is often regarded as an electron-withdrawing group; however, these fluoro-substituted PAs show a gradual red-shift from their UV-vis absorption and PL emission measurements, especially in the thin film state. In other words, the conjugation length

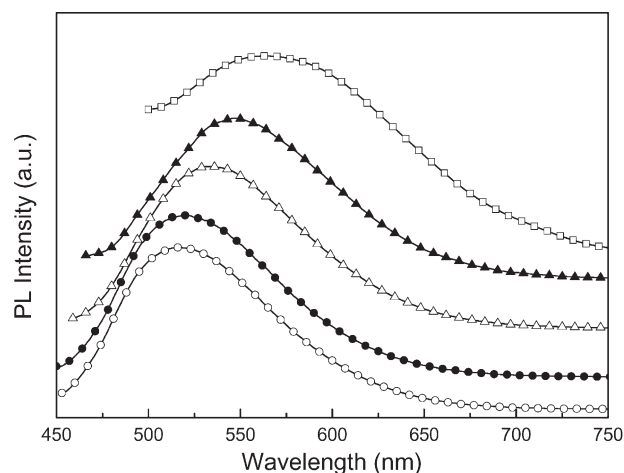


Figure 3. Photoluminescent spectra of polymers **PDPA-P** (○), **PDPA-1F** (●), **PDPA-2F** (△), **PDPA-3F** (▲), and **PDPA-5F** (□) in the thin film state.

Table 2. Optical properties and PL efficiencies of polymers **PDPA-P**, **PDPA-1F**, **PDPA-2F**, **PDPA-3F**, and **PDPA-5F**.

Polymer	UV-vis		PL		Φ_{PL}
	nm		nm		%
	Solution	Film	Solution	Film	Film
PDPA-P	430	492	423	517	55
PDPA-1F	430	494	429	519	53
PDPA-2F	437	500	433	536	44
PDPA-3F	438	533	441	547	31
PDPA-5F	480	569	473	568	4

is elongated for the PAs that contain more fluorine atoms. We speculate that this phenomenon is a result of a stacking effect. For **PDPA-P**, the pendent phenyl rings possess a torsional twist from the PA main chain that prevents close packing of neighboring polymer chains. For **PDPA-1F** to **PDPA-5F**, the fluorine atoms show a polarization force to attract each other and cause the pendent phenyl rings to stack together, which results in close packing of the main chains. With more fluorine substitutions, the extent of chain stacking increases and a red-shift in optical properties takes place.

The PL quantum efficiencies (Φ_{PL}) of these PAs were also measured and are listed in Table 2. It can be seen that the Φ_{PL} value decreases from 55% (**PDPA-P**) to 4% (**PDPA-5F**) as the number of fluorine atoms increase. The decreased Φ_{PL} value can be explained by a similar stacking effect. Since a pendent fluorophenyl group helps to stack the polymer chains together, the formation of chain aggregation results in a red-shift in the solid state. In this situation energy transfer from neighboring polymers occurs and decreases the Φ_{PL} values.

Electrochemical Analysis

Cyclic voltammetry (CV) was employed to investigate the electrochemical behaviors of the synthesized polymers and to estimate their energy levels. The oxidation process is clear and directly associated with the conjugation structure of the polymer. Figure 4 shows cyclic voltammograms of some polymers in the oxidation process. The HOMO energy level is determined from the onset of the oxidation curve (E_{ox}), which is given by

$$\text{HOMO(eV)} = -|E_{\text{ox}} + 4.4|$$

which are in the range from -5.3 to -5.73 eV. The energy gaps (EG) of materials are determined from the edge of their UV-vis absorption spectra (λ_{onset}), which is given by

$$\text{EG(eV)} = 1240/\lambda_{\text{onset}}$$

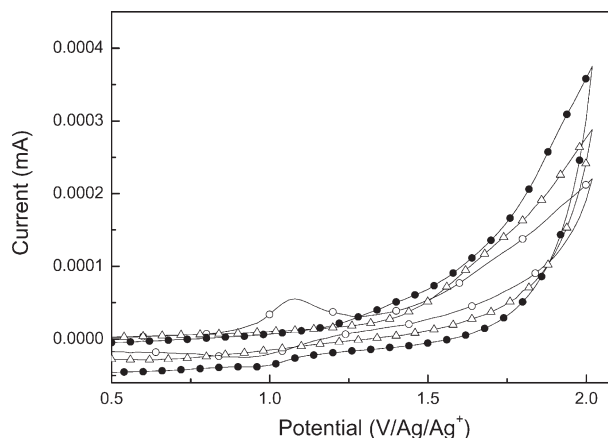


Figure 4. Cyclic voltammograms of polymers **PDPA-P** (○), **PDPA-2F** (●), and **PDPA-5F** (△).

The EG values of the synthesized PA derivatives are in the range from 2.29 to 2.67 eV. Combining the electrochemical data and UV-vis characteristics gives an estimate of the LUMO energy levels. Table 3 summarizes the HOMO, LUMO, and EG values of the five PA derivatives. By incorporating strong electron-withdrawing fluorine atoms onto the conjugated main chain, the LUMO and HOMO levels of fluorinated polymers **PDPA-1F**, **PDPA-2F**, **PDPA-3F**, and **PDPA-5F** were all lowered as compared to **PDPA-P**. Similar observations were also reported in the previous literature.^[21–23] Furthermore, the incorporation of more fluorine atoms caused a larger decrease in LUMO levels, and consequently resulted in smaller EG values. The results are in accordance with optical observations, i.e., the extent of red-shift increases with the introduction of more fluorine atoms.

Device Performance

Double-layer light-emitting diodes with the configuration of ITO/PEDOT/polymer/Ca/Al were fabricated to evaluate the EL performance of synthesized PA derivatives. The EL emission spectra of these polymers are shown in Figure 5,

Table 3. Electrochemical properties of polymers **PDPA-P**, **PDPA-1F**, **PDPA-2F**, **PDPA-3F**, and **PDPA-5F**.

Polymer	E_{ox}	HOMO	UV edge	EG	LUMO
	V	eV	nm	eV	eV
PDPA-P	0.9	-5.3	464	2.67	-2.63
PDPA-1F	1.1	-5.5	464	2.67	-2.83
PDPA-2F	1.2	-5.6	471	2.63	-2.97
PDPA-3F	1.3	-5.7	481	2.58	-3.12
PDPA-5F	1.33	-5.73	541	2.29	-3.44

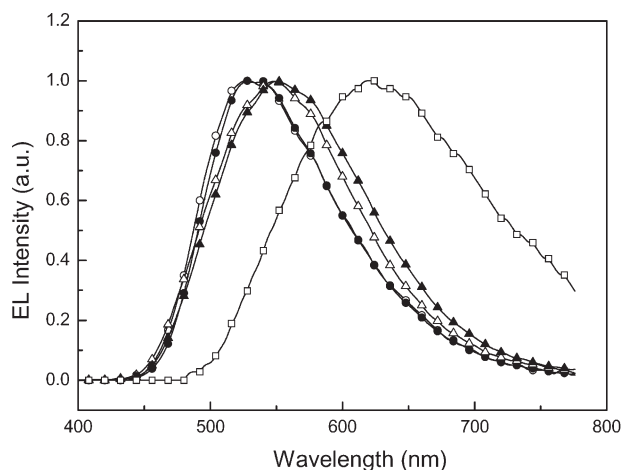


Figure 5. Electroluminescent spectra of polymers PDPA-P (○), PDPA-1F (●), PDPA-2F (△), PDPA-3F (▲), and PDPA-5F (□) in ITO/PEDOT/polymer/Ca/Al devices.

and their emission maxima are listed in Table 4. The EL emissive maxima are located from 528 to 620 nm. The CIE coordinates of five polymers are also shown in Table 4, referring to green (PDPA-P, PDPA-1F), green-yellow (PDPA-2F, PDPA-3F), and orange light (PDPA-5F). It is noted that the emission maximum of PDPA-5F is located at 620 nm, which normally refers to red light; however, its EL spectrum is pretty broad and covers a certain part of the yellow region, as shown in Figure 5. Here again the EL spectra of these PA derivatives shows a greater red-shift upon incorporating more fluorine atoms.

Table 4 also summarizes the turn-on voltage, max brightness, and max current efficiency of these devices. The turn-on voltages are quite close, ≈ 6 –7 volts. The device using PDPA-P as the active layer showed a moderate brightness of $195 \text{ cd} \cdot \text{m}^{-2}$ and current efficiency of $0.06 \text{ cd} \cdot \text{A}^{-1}$. By introducing one or two fluorine atoms on the pendent phenyl ring, the device performance was improved to some extent. PDPA-2F showed the highest brightness of $828 \text{ cd} \cdot \text{m}^{-2}$ and a current efficiency of $0.78 \text{ cd} \cdot \text{A}^{-1}$. Upon introducing more fluorine atoms, however, the device performance dropped off. The device using PDPA-5F as the active layer showed a quite low brightness

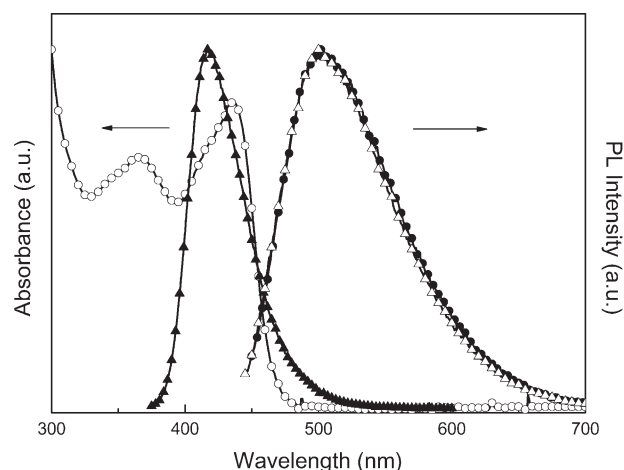


Figure 6. UV-vis spectrum of PDPA-2F (○) and PL spectra of TM-TPD (▲), PDPA-2F (●), and the blend of PDPA-2F and 10 wt.-% TM-TPD (△).

of $17 \text{ cd} \cdot \text{m}^{-2}$ and current efficiency of $0.01 \text{ cd} \cdot \text{A}^{-1}$. In the following part we chose PDPA-2F as the active material and proposed different approaches to improve its device performance.

Approaches to Highly Efficient PLEDs

To further improve the device performance of the synthesized PDPA-2F, two approaches were proposed as follows. One is based on a blend of PDPA-2F and a hole transport material TM-TPD as the active layer, while the other one is by incorporating carbazole units into the PDPA-2F backbone.

The synthesis of the copolymer PDPA-2Fcab is shown in Scheme 2. The obtained PDPA-2Fcab also has high molecular weights ($\bar{M}_n = 7.38 \times 10^5$, $\bar{M}_w = 1.09 \times 10^6$) and a relatively low PDI value of 1.48. The T_g and T_d values obtained from DSC and TGA are 228 and 406°C , respectively. The result reveals that PDPA-2Fcab is competitive with previous di-substituted PA derivatives.

Figure 6 shows the UV-visible absorption and PL emission spectra of PDPA-2F, TM-TPD, and the blend of

Table 4. Device performance of polymers PDPA-P, PDPA-1F, PDPA-2F, PDPA-3F, and PDPA-5F in ITO/PEDOT/polymer/Ca/Al devices.

Polymer	EL	$V_{\text{turn-on}}$	Max. brightness	Max. efficiency	CIE' 1931	
	nm				volt	$\text{cd} \cdot \text{m}^{-2}$
PDPA-P	528	6	195	0.06	0.36	0.54
PDPA-1F	528	6	235	0.45	0.37	0.54
PDPA-2F	540	6	828	0.78	0.39	0.54
PDPA-3F	548	7	153	0.02	0.39	0.52
PDPA-5F	620	7	17	0.01	0.54	0.45

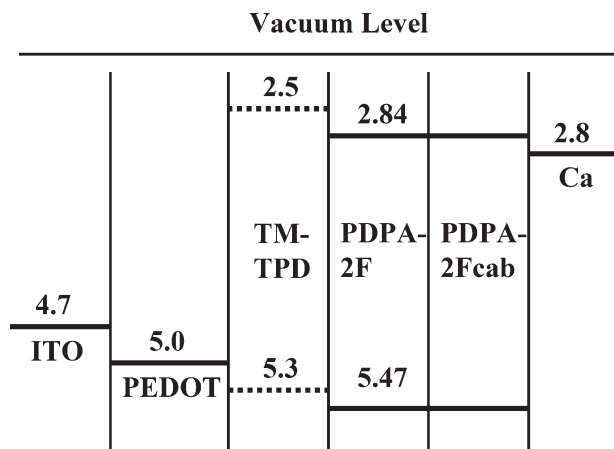


Figure 7. Energy level diagrams of PDPA-2F, TM-TPD, and PDPA-2Fcab.

90 wt.-% PDPA-2F and 10 wt.-% TM-TPD in solution or thin film state. As mentioned earlier, the UV-vis spectrum of PDPA-2F shows two absorption peaks at 365 and 435 nm, which are attributed to the $\pi-\pi^*$ inter-band transition of the main chains.^[15] The PL spectrum of TM-TPD ranges from 374 to 524 nm with an emission maximum located at 418 nm. Owing to efficient Förster transfer from TM-TPD to PDPA-2F, the emission spectrum of the blend is essentially identical to that of PDPA-2F; no emission band of TM-TPD is observed.

The energy levels of electronic states were studied by electrochemical analysis. Figure 7 presents the HOMO and LUMO energetic levels of different organic layers. According to the energy level diagram, the LUMO levels of PDPA-2F and PDPA-2Fcab are both located at -2.97 eV, which is close to the work function of the Ca cathode. The close value implies that electrons can be injected from the Ca cathode into the polymer layer easily. On the other hand, the HOMO level of TM-TPD is -5.3 eV, which is quite close to that of the ITO/PEDOT layer; the ease of hole injection is also concluded. In addition, the HOMO/LUMO levels of PDPA-2Fcab are found to be similar to those of PDPA-2F, which implies little effect of the carbazole pendent group on the photophysics of the copolymer.

Figure 8a–c shows the current density, brightness, and current efficiency versus applied voltage for different emissive polymer used in double-layer devices with the configuration of ITO/PEDOT/polymer/Ca/Al. A higher current density and lower turn-on voltage were found with increasing TM-TPD content in the PDPA-2F layer. The turn-on voltages of these devices are 5, 4, 3, and 2 volts with adding 0, 5, 10, and 20 wt.-% of TM-TPD, respectively. The result shows that the incorporation of TM-TPD improves the injection and transport of hole carriers in these devices. The device with 5 wt.-% of TM-TPD revealed a maximum current efficiency of $3.56 \text{ cd} \cdot \text{A}^{-1}$ under a

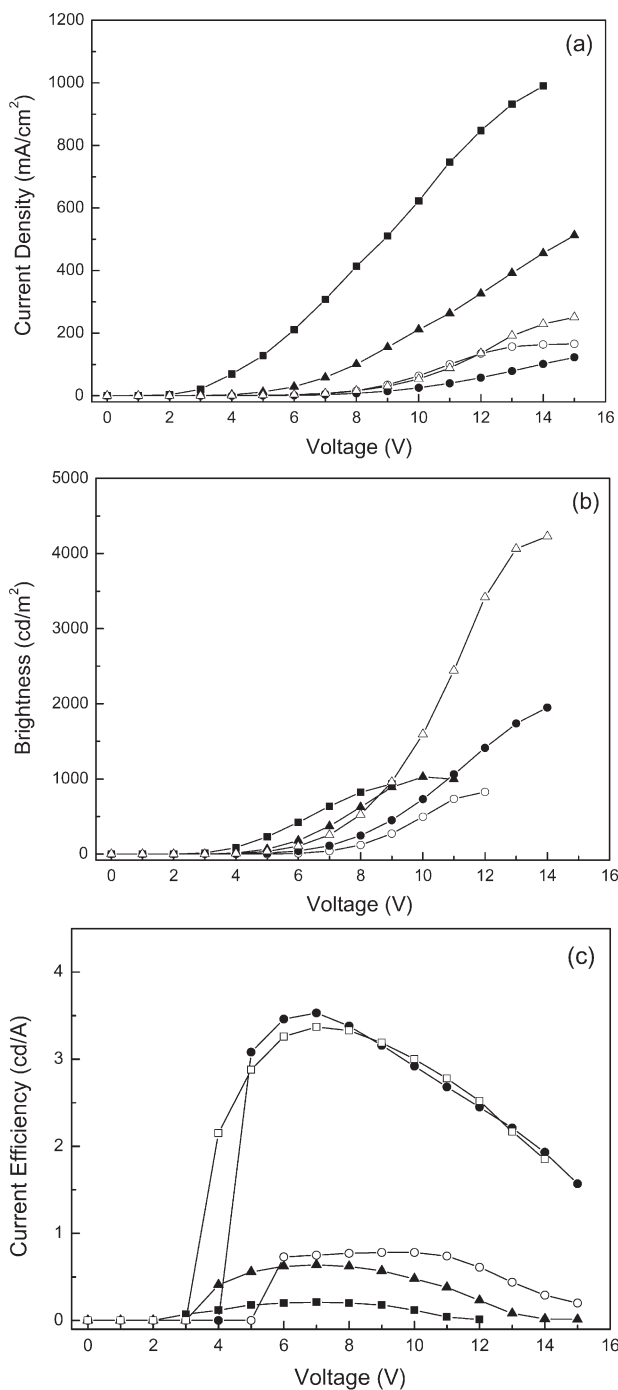


Figure 8. a) Current density, b) brightness, and c) current efficiency versus applied voltage of PDPA-2F (○), the blend of PDPA-2F and 5 wt.-% (●), 10 wt.-% (▲), and 20 wt.-% (■) of TM-TPD, and PDPA-2Fcab (△) in ITO/PEDOT/polymer/Ca/Al devices.

current density of $3 \text{ mA} \cdot \text{cm}^{-2}$ at 7 V, and a maximum brightness of $1950 \text{ cd} \cdot \text{m}^{-2}$ at 14 V. However, the device with 20 wt.-% of TM-TPD showed a decreased performance, i.e., a maximum brightness of $934 \text{ cd} \cdot \text{m}^{-2}$ and a maximum current efficiency of $0.21 \text{ cd} \cdot \text{A}^{-1}$ were found.

Table 5. Device performance of hybrid PDPA-2F + TM-TPD and pristine PDPA-2Fcab in ITO/PEDOT/polymer/Ca/Al devices.

Polymer	EL	$V_{\text{turn-on}}$	Max. brightness	Max. efficiency	CIE' 1931	
	nm	volt	$\text{cd} \cdot \text{m}^{-2}$	$\text{cd} \cdot \text{A}^{-1}$	x	Y
PDPA-2F + 5% TM-TPD	536	4	1950	3.56	0.35	0.54
PDPA-2F + 10% TM-TPD	532	3	996	0.64	0.35	0.52
PDPA-2F + 20% TM-TPD	532	3	934	0.21	0.32	0.54
PDPA-2Fcab	532	4	4230	3.37	0.35	0.54

We attributed this observation to the result of an excess amount of TM-TPD. The crystallization of TM-TPD was performed and observed by optical microscopy, which resulted in lower device performance. Turning to PDPA-2Fcab, the turn-on voltage of the device is 3.5 V. It showed a maximum current efficiency of $3.37 \text{ cd} \cdot \text{A}^{-1}$ under a current density of $7 \text{ mA} \cdot \text{cm}^{-2}$ at 7 V. A maximum brightness of $4230 \text{ cd} \cdot \text{m}^{-2}$ under a current density of $228 \text{ mA} \cdot \text{cm}^{-2}$ at 14 V was observed. The device performance of PDPA-2Fcab is approximately 100 times higher than that formerly of PDPA.^[7] The device performance of the hybrid PDPA-2F + TM-TPD and pristine PDPA-2Fcab is summarized in Table 5.

In order to comprehend the difference in the performance of these devices, we fabricated several hole- and electron-only devices to compare current densities (and thus mobility) of two carriers inside the polymer layer.^[17] The device structure of a typical hole-only device is ITO/PEDOT/polymer/Au. In this device, hole injection is predominant, while electrons are difficult to inject from the Au cathode into the polymer layer. Moreover, an electron-only device is fabricated with the configuration of ITO/Al/polymer/Ca/Al. In this case electron injection is

relatively major and the hole would be blocked between the ITO and metal Al. The current density–electrical field characteristics of PDPA-2F, the blend of PDPA-2F and 5 wt.-% of TM-TPD, and PDPA-2Fcab are shown in Figure 9. For PDPA-2F, the current density of electrons is higher than that of holes by one order at the same electric field, which indicates that PDPA-2F is an electron-transporting material. For the blend of PDPA-2F and TM-TPD, the hole current is increased and the difference in current density of the holes and electrons is decreased as compared with pristine PDPA-2F. The results described above help to explain the improvement of device performance of PDPA-2F by adding a hole-transporting material TM-TPD. For PDPA-2Fcab, the hole-transporting moiety of carbazole was incorporated into the polymer chain, and phase separation and crystallization phenomena can be diminished. The current densities of the holes and electrons are close to each other at various electrical fields, which indicates a charge balance of two carriers inside the polymer layer. The polymer PDPA-2Fcab showed the best device performance among the PA derivatives synthesized in this work and in the literature.

Figure 10 illustrates the EL spectra of pristine PDPA-2F, the blend of PDPA-2F and TM-TPD, and PDPA-2Fcab alone. The emissive maxima of three materials are located at same position, and the shape of the three EL spectra are pretty similar, which suggests that the emissive behavior of PDPA-2F is not affected by the incorporation of TM-TPD or carbazole moieties significantly. The CIE'1931 coordinates are located at (0.35, 0.54), which refers to a yellowish-green color.

Conclusion

In summary, a novel series of fluorophenyl PA derivatives were successfully synthesized and characterized. These PA derivatives show good thermal stability and solubility in common organic solvents. Optical studies reveal that incorporating more fluorine atoms on the pendent phenyl ring results in a greater red-shift in the UV-vis absorption and PL emission. However, the PL efficiency decreases with increasing the number of fluorine atoms.

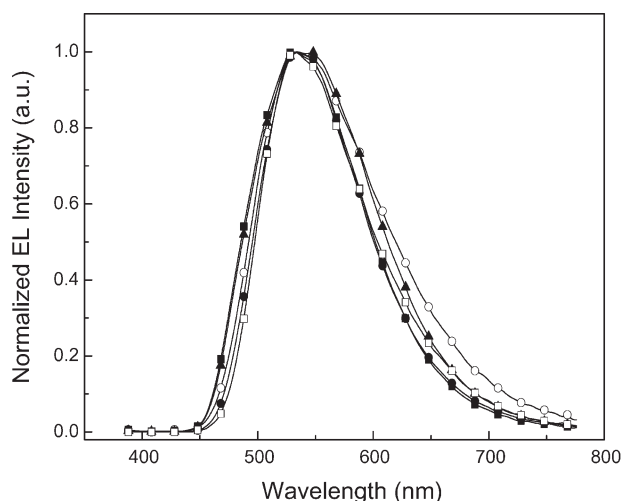


Figure 10. Normalized EL spectra of the devices using PDPA-2F (○), the blend of PDPA-2F and 5 wt.-% (●), 10 wt.-% (▲), and 20 wt.-% (■) of TM-TPD, and PDPA-2Fcab (△) as active layers.

We also investigated two approaches to achieve high brightness and efficiency of electroluminescent devices by blending with TM-TPD or by incorporating carbazole moieties into polymer chains. The hole injection and transport can be improved by two approaches according to the observation of lowered turn-on voltage and electrical properties. A well-established charge balance of holes and electrons in **PDDPA-2Fcab** was studied from hole- and electron-only devices. To the best of our knowledge, the synthesized **PDDPA-2Fcab** has shown the best electroluminescent properties so far. The results reveal that these materials are promising candidates for PLED applications.

Acknowledgements: The authors are grateful to the *National Science Council of the Republic of China* (NSC 95-2221-E-009-161-MY3) and *Ministry of Education* (MOE ATU Program) for its financial support of this work.

Received: September 24, 2008; Revised: October 30, 2008;
Accepted: October 30, 2008; DOI: 10.1002/macp.200800467

Keywords: conjugated polymers; light-emitting diodes; metathesis; polyacetylenes

- [1] J. H. Burroughes, D. D. C. Bradley, A. R. Brown, R. N. Marks, K. Mackay, R. H. Friend, P. L. Burn, A. Kraft, A. B. Holmes, *Nature* **1999**, *347*, 539.
- [2] G. Gustatsson, Y. Gao, G. M. Treacy, F. Klavetter, N. Colaneri, A. J. Heeger, *Nature* **1992**, *357*, 477.
- [3] H. E. Katz, *J. Mater. Chem.* **1997**, *7*, 369.
- [4] S. N. Chen, A. J. Heeger, Z. Kiss, A. G. MacDiarmid, S. C. Gau, D. L. Peebles, *Appl. Phys. Lett.* **1980**, *36*, 96.
- [5] C. K. Chiang, S. C. Gau, C. R. Fincher, Jr., Y. W. Park, A. G. MacDiarmid, A. J. Heeger, *Appl. Phys. Lett.* **1978**, *33*, 18.
- [6] S. Hirakawa, T. Masuda, K. Takeda, "The Chemistry of Tripolebonded Functional Groups", S. Patai, Ed., John Wiley & Sons, New York 1994.
- [7] K. Tada, R. Hidayat, M. Hirohata, M. Teraguchi, T. Masuda, K. Yoshino, *Jpn. J. Appl. Phys.* **1996**, *35*, L1138.
- [8] R. Hidayat, M. Hirohata, K. Tada, M. Teraguchi, T. Masuda, K. Yoshino, *Jpn. J. Appl. Phys.* **1997**, *36*, 3740.
- [9] K. Nanjo, S. A. Karim Abdul, R. Nomura, T. Wada, H. Sasabe, T. Masuda, *J. Polym. Sci., Part A: Polym. Chem.* **1999**, *37*, 277.
- [10] F. Sanda, T. Nakai, N. Kobayashi, T. Masuda, *Macromolecules* **2004**, *37*, 2703.
- [11] P. P. Lee, Y. Geng, H. S. Kwok, B. Z. Tang, *Thin Solid Films* **2000**, *363*, 149.
- [12] Z. Xie, Jacky, W. Y. Lam, Y. Dong, C. Qiu, H. Kwok, B. Z. Tang, *Opt. Mater.* **2002**, *21*, 231.
- [13] J. C. Chen, Z. Xie, Jacky, W. Y. Lam, C. C. W. Law, B. Z. Tang, *Macromolecules* **2003**, *36*, 1108.
- [14] J. W. Y. Lam, B. Z. Tang, *J. Polym. Sci., Part A: Polym. Chem.* **2003**, *41*, 2607.
- [15] C. H. Ting, C. S. Hsu, *Jpn. J. Appl. Phys.* **2001**, *40*, 5342.
- [16] C. H. Ting, J. T. Chen, C. S. Hsu, *Macromolecules* **2002**, *35*, 1180.
- [17] C. H. Huang, S. H. Yang, K. B. Chen, C. S. Hsu, *J. Polym. Sci., Part A: Polym. Chem.* **2006**, *45*, 519.
- [18] S. T. Wu, J. D. Margerum, M. S. Ho, B. M. Fung, C. S. Hsu, *Mol. Cryst. Liq. Cryst.* **1995**, *261*, 79.
- [19] J. W. Yip, H. Peng, M. Haussler, R. Zheng, B. Z. Tang, *Mol. Cryst. Liq. Cryst.* **2004**, *415*, 43.
- [20] A. Beganskiene, P. Adomenas, R. Sirutkaitis, Y. Goto, *Mol. Cryst. Liq. Cryst.* **1995**, *260*, 273.
- [21] S. B. Heidenhain, Y. Sakamoto, T. Suzuki, A. Miura, H. Fujikawa, T. Mori, S. Tokito, Y. Taga, *J. Am. Chem. Soc.* **2000**, *122*, 10240.
- [22] Y. Jin, J. Kim, S. Lee, J. Y. Kim, S. H. Park, K. Lee, H. Suh, *Macromolecules* **2004**, *37*, 6711.
- [23] A. Facchetti, M. H. Yoon, C. L. Stern, H. E. Katz, T. J. Mark, *Angew. Chem. Int. Ed.* **2003**, *42*, 3900.